🔓 OPEN ACCESS

Utilizing developmental dynamics for evolutionary prediction and control

Lisandro Milocco[a,1] 🔟 and Tobias Uller[a] 🔟

Understanding, predicting, and controlling the phenotypic consequences of genetic and environmental change is essential to many areas of fundamental and applied biology. In evolutionary biology, the generative process of development is a major source of organismal evolvability that constrains or facilitates adaptive change by shaping the distribution of phenotypic variation that selection can act upon. While the complex interactions between genetic and environmental factors during development may appear to make it impossible to infer the consequences of perturbations, the persistent observation that many perturbations result in similar phenotypes indicates that there is a logic to what variation is generated. Here, we show that a general representation of development as a dynamical system can reveal this logic. We build a framework that allows predicting the phenotypic effects of perturbations, and conditions for when the effects of perturbations of different origins are concordant. We find that this concordance is explained by two generic features of development, namely the dynamical dependence of the phenotype on itself and the fact that all perturbations must affect the developmental process to have an effect on the phenotype. We apply our theoretical framework to classical models of development and show that it can be used to predict the evolutionary response to selection using information of plasticity and to accelerate evolution in a desired direction. The framework we introduce provides a way to quantitatively interchange perturbations, opening an avenue of perturbation design to control the generation of variation.

evo-devo | plasticity | evolvability | dynamical systems | prediction

A complete theory of organismal evolution requires a theory of phenotypic variation, a theory of natural selection, and a theory of heredity. While tremendous advances have been made in the last century to understand the two latter pillars of Darwinian evolution, a theory for the generation of phenotypic variation remains elusive.

The process that generates variation in morphology, physiology, and behavior is known as development in the broad sense (1). Notoriously complex and nonlinear interactions between genes, cells, tissues, and environmental factors during development make it difficult to grasp the phenotypic consequences of genetic and environmental perturbations. Indeed, the diversity and complexity of developmental systems could be taken as evidence that a priori inference of the consequences of perturbations rarely will be feasible. A pessimistic conclusion is therefore that the best one could hope for is to demonstrate that generative processes in principle can impact evolutionary trajectories (2–4), while studies that demonstrate how development affects evolution will remain a collection of idiosyncratic case studies (5–7). This perception that generative processes are intrinsically unpredictable and that selection is the only reliable force in evolution is also reflected in biotechnology and medicine, where attempts to direct evolutionary processes emphasize control over selective regimes rather than control over generative processes.

In this paper, we provide a more optimistic perspective by addressing a particular problem concerning the generation of variation and its implications for evolution: the relationship between the phenotypic effects of different genetic and environmental perturbations. Genetic and environmental effects on phenotypic variation have often been considered to be independent, as assumed in models of quantitative genetics where phenotypes are represented as the sum of uncorrelated genetic and environmental contributions (8, 9). However, since both genetic and environmental perturbations are channeled through the same developmental system, it is unlikely that this assumption generally holds true (10, 11). It is indeed well known that environmental change occasionally induces phenotypes that resemble genetic mutants [e.g., melanism in butterflies (12)], and it has been shown that plastic responses are biased toward phenotype

Significance

Variation in traits is the raw material for evolution. Yet, the complexity of development makes it daunting to predict, control, and engineer evolution by manipulating the generation of phenotypic variation. By representing development as a dynamical system, we build a bottom–up theoretical framework to predict the effects of genetic and environmental perturbations on the resulting traits. We find conditions for when different perturbations result in concordant changes in the traits and show how this can be used for evolutionary prediction and to steer evolution in a preferred direction.

Author affiliations: [a]Department of Biology, Lund University, 223 62 Lund, Sweden

dimensions with high additive genetic variation (13), but the existing body of work is mostly a collection of empirical observations.

If genes and environments are to some degree equivalent, or interchangeable, as sources of phenotypic variation, this could have important consequences for understanding and predicting evolution, and eventually controlling it. In particular, gene–environment interchangeability implies that there is a formal connection between evolvability and plasticity. Evolvability can be defined as the capacity to generate phenotypic variation in response to genotypic variation (14), while plasticity refers to the same capacity for phenotypic variation in response to environmental variation. If genetic and environmental perturbations are interchangeable to some degree, the evolution of plasticity may shape evolvability and vice versa, and information of one can reveal features of the other (15). Previous theoretical work has suggested that such a relationship between plasticity and evolvability does exist (16–22), but there is no general framework to explicitly define the conditions for when this relationship should be expected or to study its evolutionary implications. Such understanding would enable designing combinations of perturbations to drive the developmental system to a desired state, thus controlling the generation of variation.

The aim of this paper is to introduce a conceptual framework to understand when perturbations of different origins will cause shifts in phenotype in similar directions in trait space. We illustrate this phenomenon of alignment using in silico experiments of reaction–diffusion models and gene regulatory networks. We show how the theory can be used i) to predict the concordance of phenotypic effects of perturbations of different origins, such as two different genetic perturbations, or a genetic and an environmental perturbation, ii) to estimate the effects of mutations on the phenotype, iii) to infer evolvability using information of plasticity, and iv) to accelerate evolution in a desired direction. This ability to convert information from plastic responses into information about evolutionary potential, and vice versa, could have applications in diverse areas concerned with the phenotype, including developing solutions to environmental and societal challenges using biotechnological engineering.

Results

The results are presented in sections. First, we introduce a general representation of development as a dynamical system. Second, we develop the formalism to study the phenotypic effect of a single perturbation. Third, we study the alignment between perturbations of different origins (e.g., genetic and environmental). Finally, we apply the theoretical framework to classical models of development, namely reaction–diffusion models and gene regulatory networks, and show how it can be used for evolutionary understanding, prediction, and even control. We note that these examples have been chosen for illustrative purposes, but the applicability of the framework is not confined to them.

A General Representation of Development as a Dynamical System. Mathematical models of development usually consist of a representation of the phenotype and a set of rules of how this phenotype changes through developmental time, for example, through the interaction among different components of the system. Examples of such models include reaction–diffusion models (e.g., ref. 23), gene regulatory networks (e.g., ref. 24), and models of morphogenesis (e.g., ref. 25). These models are commonly given mathematically as differential equations which

are numerically integrated over time to simulate a developmental trajectory, which is the change in the phenotypic values through developmental time. Following this body of work (26, 27), we take the general representation of development given by

$$\dot{\boldsymbol{x}} = \boldsymbol{f}(t, \boldsymbol{x}, \lambda), \quad \boldsymbol{x}(t_0) = \boldsymbol{x}_0, \quad [1]$$

where $\boldsymbol{x} = (x_1, x_2, ..., x_n)$ is a vector composed of n variables that we refer to as *states*, with each state x_i representing a different aspect of the phenotype that is relevant to describe the system's behavior and that changes during developmental time (e.g., the expression level of a given gene); $\dot{\boldsymbol{x}}$ is the time derivative of $\boldsymbol{x}$, which gives the temporal change in the states; t is developmental time; $\boldsymbol{f}$ is a developmental function determining the rules of how the states change in time; $\boldsymbol{x}_0$ are the state values at initial time t_0, known as the initial conditions; and $\lambda = (\lambda_1, \lambda_2, ..., \lambda_p)$ are developmental parameters, which can be genetic or environmental (e.g., the affinity of a cofactor modulating downstream gene expression, or temperature during developmental time). Unlike states, developmental parameters do not change dynamically.

Eq. **1** captures two central properties of development which will be important to derive the results presented later. The first of these central aspects is that development depends at each step on the preexisting phenotype. This is mathematically captured by the fact that the change in the states at each time, given by $\dot{\boldsymbol{x}}$, is itself a function of the states $\boldsymbol{x}$ at that time. This means that the phenotype at any given time is both the effect of earlier and the cause of later developmental changes. This feedback of the phenotype on itself makes development a *dynamical* phenomenon rather than a *static* one (11, 28), where the ways in which the phenotype can and cannot change at a given time depend on the state of the phenotype at that time. Examples of this historicity of development include the sequential determination of cell fate (29) and sensitivity windows, where the same perturbation results in a phenotypic effect only for responsive phenotypes at specific times during development (30).

The second important aspect of development highlighted by Eq. **1** is that changes in any of the developmental parameters λ have an effect on the states $\boldsymbol{x}$ through the same function $\boldsymbol{f}$. In other words, any perturbation in the developmental parameters has to be channeled through the developmental function to result in a change in the states. As we show below, this functional dependence of development on the parameters (10, 11) is fundamental to study the alignment of the effects of perturbations with different origins.

While for the rest of the manuscript we develop the framework to study alignment when the phenotypes of interest are the state variables $\boldsymbol{x}$, the framework can also be extended to study alignment when phenotypes are a function of these state variables, as explained in *Appendix A*.

The Effect of a Perturbation on One Developmental Parameter. We are interested in studying how a given developmental trajectory is affected by a perturbation in one of the developmental parameters. We begin with a system with a single developmental parameter (i.e., $\lambda = \lambda$), and we extend the results to multiple parameters later. Further, we will assume that the developmental function $\boldsymbol{f}$ is smooth, having continuous partial first derivatives. While limiting the applicability of the framework, a large number of models of development fulfill this condition as we show below.

The study of perturbations is always comparative: Perturbations must be studied with respect to an unperturbed reference. We thus need to define a reference developmental trajectory from

which to study deviations from. We define λ^* as the reference value for the developmental parameter (i.e., corresponding to an organism with the wild-type genotype in standard environmental conditions). The developmental trajectory of the reference, unperturbed developmental system is thus given as the unique solution of Eq. 1 for $\lambda = \lambda^*$, which we denote $\boldsymbol{x}(t, \lambda^*)$, as shown in Fig. 1.

We are interested in the direction in which the reference developmental trajectory will change when we introduce a small perturbation to λ^*. This type of study is known as *sensitivity analysis* in dynamical systems theory (31). The direction of change is given by

$$\boldsymbol{s}_\lambda(t) = \left.\frac{\partial \boldsymbol{x}(t, \lambda)}{\partial \lambda}\right|_{(t, \lambda^*)}. \qquad [2]$$

The vector $\boldsymbol{s}_\lambda(t)$ is known as the *sensitivity vector* [or *function*, (31)], and it is a vector of length n containing the partial derivatives of the states $x_1, x_2, \ldots, x_n$ with respect to the parameter λ, evaluated at the reference value λ^* and at time t. This vector then tells us how we expect the states to change for a small change in the developmental parameter at each time t. For small perturbations, we can predict the perturbed developmental trajectory using

$$\boldsymbol{x}(t, \lambda) \approx \boldsymbol{x}(t, \lambda^*) + \boldsymbol{s}_\lambda(t)(\lambda - \lambda^*), \qquad [3]$$

which tells us that the perturbed developmental trajectory $\boldsymbol{x}(t, \lambda)$ will differ from the reference, unperturbed trajectory $\boldsymbol{x}(t, \lambda^*)$ by an amount proportional to the difference $\lambda - \lambda^*$, with direction determined by the vector $\boldsymbol{s}_\lambda(t)$. Eq. 3 resembles a first-order Taylor approximation, and is only locally valid (i.e., for values of λ close to λ^*). While additional terms of the Taylor expansion could in principle be added to improve accuracy, we focus here on the linear approximation shown in Eq. 3.

Calculating $\boldsymbol{s}_\lambda(t)$ is not straightforward since we do not know the explicit relationship between the states $\boldsymbol{x}$ and the parameter λ. We show in *Appendix B* (see also ref. 31) that $\boldsymbol{s}_\lambda(t)$ can be obtained as the unique solution to

$$\dot{\boldsymbol{s}}_\lambda(t) = A(t, \lambda^*)\boldsymbol{s}_\lambda(t) + \boldsymbol{b}_\lambda(t, \lambda^*), \quad \boldsymbol{s}_\lambda(t_0) = 0 \qquad [4]$$

$$A(t, \lambda^*) = \left.\frac{\partial \boldsymbol{f}(t, \boldsymbol{x}, \lambda)}{\partial x}\right|_{\boldsymbol{x}(t, \lambda^*)}, \quad \boldsymbol{b}_\lambda(t, \lambda^*) = \left.\frac{\partial \boldsymbol{f}(t, \boldsymbol{x}, \lambda)}{\partial \lambda}\right|_{\boldsymbol{x}(t, \lambda^*)}.$$

The matrix $A(t, \lambda^*)$ is known as the Jacobian matrix and summarizes the relationship between $\boldsymbol{f}$ and $\boldsymbol{x}$. Note that this
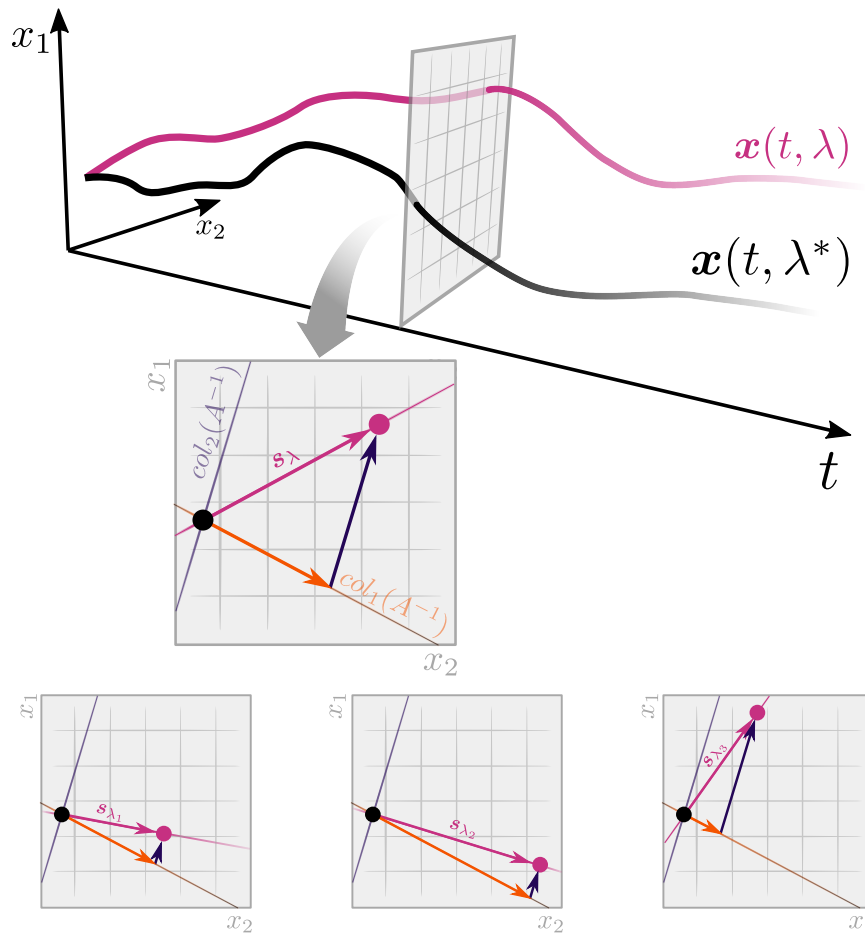
Fig. 1. A general framework to study the phenotypic effects of perturbations of different origins. On *Top*, the reference developmental trajectory $\boldsymbol{x}(t, \lambda^*)$ in black and the perturbed trajectory $\boldsymbol{x}(t, \lambda)$ in purple through developmental time t. The panel in the *Middle* shows that, at any given time, the effect of the perturbation on the trajectory, given by the sensitivity vector $\boldsymbol{s}_\lambda(t)$ is a linear combination of the columns of the matrix $A^{-1}(t, \lambda^*)$. The three panels at the *Bottom* show the sensitivity vectors for different perturbations at a given developmental time are linear combinations of the columns of the same A^{-1}. $\boldsymbol{s}_{\lambda_1}$ and $\boldsymbol{s}_{\lambda_2}$ are largely aligned, but not $\boldsymbol{s}_{\lambda_3}$.

Jacobian does not depend on what parameter λ is perturbed. The relationship between $\boldsymbol{f}$ and λ is captured by the vector $\boldsymbol{b}_\lambda(t, \lambda^*)$. In this way, if we know the function $\boldsymbol{f}$, then we can calculate $A(t, \lambda^*)$ and $\boldsymbol{b}_\lambda(t, \lambda^*)$, and jointly solve numerically Eqs. **1** and **4** to obtain $\boldsymbol{s}_\lambda(t)$, which is the vector of interest.

Under the assumption that the Jacobian is invertible, we can get the simplified expression

$$\boldsymbol{s}_\lambda(t) = A^{-1}(t, \lambda^*) \underbrace{(\dot{\boldsymbol{s}}_\lambda(t) - \boldsymbol{b}_\lambda(t, \lambda^*))}_{\tilde{\boldsymbol{b}}_\lambda(t, \lambda^*)} \qquad [5]$$

$$= col_1(A^{-1})\tilde{b}_{\lambda,1} + col_2(A^{-1})\tilde{b}_{\lambda,2} + \cdots + col_n(A^{-1})\tilde{b}_{\lambda,n},$$

where $col_i(A^{-1})$ is the i-th column of $A^{-1}(t, \lambda^*)$ and $\tilde{b}_{\lambda,i}$ is the i-th element of vector $\tilde{\boldsymbol{b}}_\lambda$. This means that the sensitivity vector at a given time $\boldsymbol{s}_\lambda(t)$ can be expressed as a linear combination of the columns of $A^{-1}(t, \lambda^*)$ with weights determined by the elements of $\tilde{\boldsymbol{b}}_\lambda(t, \lambda^*)$. This result is shown graphically in Fig. 1, and provides a basis to study alignment as explained in the next section. Note that $\tilde{\boldsymbol{b}}_\lambda(t, \lambda^*)$ reduces to $-\boldsymbol{b}_\lambda(t, \lambda^*)$ if $\|\boldsymbol{b}_\lambda(t, \lambda^*)\| \gg \|\dot{\boldsymbol{s}}_\lambda(t)\|$, with $\|.\|$ the Euclidean norm. This is the case for an organism that has reached steady state (e.g., adulthood).

Alignment between the Effects of Perturbations of Different Origin. We now use the formalism introduced above to study the relationship between the phenotypic effects of perturbations of different origins. Given two developmental parameters, we say that their effects are *totally aligned* if the associated sensitivity vectors have an angle of $0°$, meaning that the two perturbations result in phenotypic changes in exactly the same direction. More generally, we say that there is some degree of alignment if the two sensitivity vectors have an angle that is significantly smaller, at a given confidence level, than the distribution of angles between independent random vectors of the same dimension—which approaches $90°$ as the number of dimensions increases.

Fig. 1 gives an example for three developmental parameters λ_1, λ_2, and λ_3, which can correspond for example to the affinity of a cofactor modulating gene expression (genetic parameter), temperature, and salinity (environmental parameters), respectively. The effects of modifying each of those parameters at time t is given by the vectors $\boldsymbol{s}_{\lambda_1}(t)$, $\boldsymbol{s}_{\lambda_2}(t)$, and $\boldsymbol{s}_{\lambda_3}(t)$, and the angles between them determine alignment. From Eq. **5**, we know that all of these sensitivity vectors can be written as linear combinations of the columns of the same matrix, the inverse of the Jacobian $A^{-1}(t, \lambda^*)$, where each column is weighted by the elements of $\tilde{\boldsymbol{b}}_\lambda$ (note that we omit the arguments (t, λ^*) when it is clear from context for readability). This provides the basis to derive sufficient conditions for alignment between the effects of different perturbations; if two perturbations have a dominant component in the direction of the same column of the inverse of the Jacobian, then these perturbations will be aligned. That is, there will be some degree of alignment between perturbing λ_1 and λ_2 if there is an i such that $\|col_i(A^{-1})\tilde{b}_{\lambda,i}\| \gg \|\sum_{j \neq i} col_j(A^{-1})\tilde{b}_{\lambda,j}\|$ for $\lambda = \lambda_1, \lambda_2$. Furthermore, there will be total alignment between the perturbations if $\tilde{\boldsymbol{b}}_{\lambda_1}$ and $\tilde{\boldsymbol{b}}_{\lambda_2}$ are proportional.

The illustrative example in Fig. 1 shows that $\boldsymbol{s}_{\lambda_1}(t)$ and $\boldsymbol{s}_{\lambda_2}(t)$ are largely aligned because they both have a large component in the direction of the first column and a small component in the direction of the second column of the inverse of the Jacobian. $\boldsymbol{s}_{\lambda_3}(t)$ is not aligned with the other two vectors, since it has a large component in the second rather than first column. We

further note that the conditions given above for alignment are sufficient but not necessary. Indeed, there can be a large degree of alignment according to our definition when the inverse of the Jacobian has columns that are similar to each other.

We highlight that the measurement of the angle between sensitivity vectors can be done at each time t of development, and therefore the measured alignment between the effects of perturbations can change in time—since the sensitivity vectors themselves can change during development. This means that if two perturbations produce similar phenotypic effects, but act at different times separated by a developmental window, the framework will measure low alignment during this window and increased alignment afterward.

The two components of the sensitivity vectors, namely $A^{-1}(t, \lambda^*)$ and $\tilde{b}_{\lambda,i}$, are related to the two key aspects of development highlighted by Eq. **1**. The first of these aspects—the historicity of development—is related to matrix $A^{-1}(t, \lambda^*)$, the inverse of the Jacobian which summarizes the relationship between $\boldsymbol{f}$ and $\boldsymbol{x}$. This matrix determines the structure for phenotypic changes, since its columns provide the directions in which the phenotype is able to respond to a perturbation. These directions are independent of the nature of the perturbation itself and are determined by the capabilities of the responsive phenotype at that time. The second relevant aspect of development highlighted by Eq. **1** is the fact that developmental parameters λ appear in the same developmental function $\boldsymbol{f}$. This is related to the other component of the sensitivity vector, the weights $\tilde{b}_{\lambda,i}$, that depend on the relationship between $\boldsymbol{f}$ and λ. In this way, alignment will be determined by how the developmental parameters affect the specific developmental function $\boldsymbol{f}$ to which the general framework is applied. In the extreme case that two developmental parameters affect exactly the same aspects of $\boldsymbol{f}$, then there will be total alignment. On the other extreme, if two parameters affect totally distinct aspects of $\boldsymbol{f}$ (e.g., they affect two different developmental modules) then we should not expect alignment in general. Between these extremes, different degrees of similarity in how developmental parameters affect developmental dynamics will result in different degrees of alignment as a result of perturbations in those parameters. Even some degree of alignment can be useful for evolutionary applications, and the framework allows to quantitatively measure this degree as we show below.

In the next sections, we apply this general framework to well-known models of development, and use it to make evolutionary prediction and control. We highlight here that these examples are for illustrative purposes, but the general framework can be applied to any developmental function of the form given in Eq. **1**. We thus make no a priori assumptions about the structure of the developmental function $\boldsymbol{f}$.

Alignment in a Reaction–Diffusion Model. Reaction–diffusion models are a set of models of pattern-formation that have been widely used to represent diverse developmental processes, including digit formation and hair follicle placement (23, 32–34). These models consist of a physical representation of the tissue and a set of molecules called morphogens. Morphogens diffuse and interact within the tissue, leading to the emergence of patterns as they accumulate in specific spatial regions. Here, we will use one of these reaction–diffusion models known as the Gray–Scott model (35) to illustrate how we can study the alignment of phenotypic effects of different origins using the framework introduced in the previous sections.

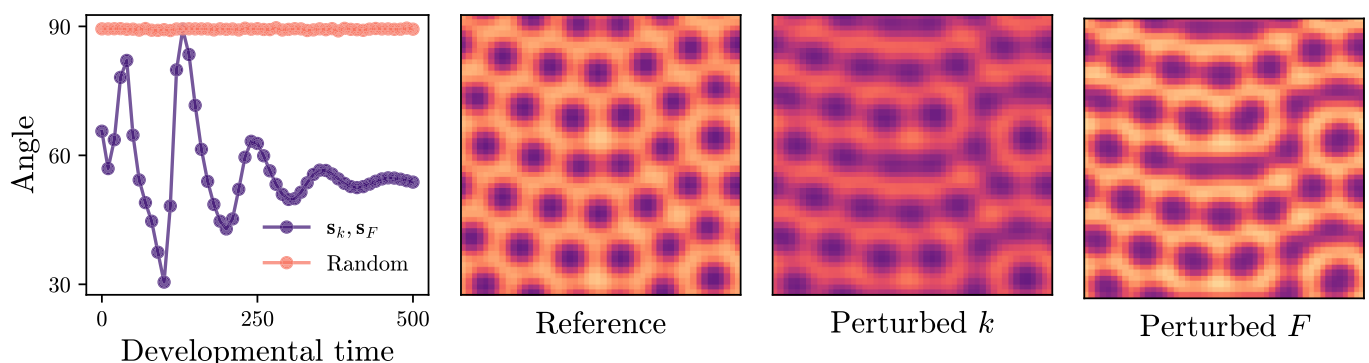The developmental function $\boldsymbol{f}$ for the Gray–Scott model is given by

$$\dot{x}_1 = D_1 \nabla^2 x_1 - x_1 x_2^2 + F(1 - x_1),$$
$$\dot{x}_2 = D_2 \nabla^2 x_2 + x_1 x_2^2 - (F + k)x_2, \tag{6}$$

where x_1 and x_2 are the cellular concentrations of morphogen 1 and 2, respectively, D_1 and D_2 are their diffusion rates to neighboring cells, ∇^2 is the Laplacian operator, F is the production rate of morphogen 1, and k is the rate of degradation of morphogen 2. These parameters have been shown to have genetic basis in some systems (23, 36), so the perturbations on these parameters can be understood as resulting from different genetic changes. We will study the alignment between the phenotypic effects of perturbing the developmental parameters k and F.

We represent a portion of embryonic tissue as a grid of 50×50 cells (details of the simulations are given in *Materials and Methods*). In each of these cells, there is a given amount of the two morphogens, so the total number of states in the system is $50 \times 50 \times 2 = 5,000$. Diffusion of the morphogens occurs between neighboring cells. The simulation is done for a window of time of $t = 5,000 \times h$ where $h = 0.1$ is the integration step. We start from initial conditions shown in *SI Appendix*, Fig. S1, and use the reference parameters values $D_1^* = 0.32$, $D_2^* = 0.06$, $k^* = 0.06$ and $F^* = 0.032$. We calculate $\boldsymbol{s}_k(t)$ and $\boldsymbol{s}_F(t)$ by jointly integrating Eq. **4**.

Fig. 2 shows that the angle between $\boldsymbol{s}_k(t)$ and $\boldsymbol{s}_F(t)$ remains around $50°$. This means that $\boldsymbol{s}_k(t)$ and $\boldsymbol{s}_F(t)$ are partially aligned, since this angle is significantly smaller than the angle between random vectors of the dimension of the sensitivity vectors, which is $90°$. This implies that the phenotypic effects of perturbing k and F should be similar.

We test the analytical prediction of alignment by simulating perturbed systems. We run simulations with small perturbations in the developmental parameters (i.e., $k = k^* + \Delta k$ and $F = F^* + \Delta F$), and compare the resulting phenotypes. Fig. 2 shows that the phenotypic effects of either a decrease in k or an increase in F are largely aligned, resulting in the formation of *connected dots* rather than *dots* as in the reference, unperturbed phenotype. Note that since the angle between $\boldsymbol{s}_k(t)$ and $\boldsymbol{s}_F(t)$ is not $0°$, we should not expect the perturbed phenotypes to be identical.

Alignment in a Gene Regulatory Network. We now use the general framework to study the alignment between the phenotypic effects of perturbation with different origins in a gene regulatory network. In this section, we derive analytical results and test them using simulations. In the next section, we use the knowledge of alignment to connect plasticity and evolvability.

We use a common representation of gene regulatory networks found in the literature (19, 24) with continuous representation of time as assumed in Eq. **1** (e.g., ref. 22). In the conventional formulation of these models, the phenotypes are the expression levels of n transcription factors that regulate each other's expression (but see *Appendix A* for a possible extension). We represent these phenotypes as states $\boldsymbol{x} = (x_1, x_2, \ldots, x_n)$, with x_i being the expression level of the i-th gene. The function $\boldsymbol{f}$ giving the change in the states during development for this example is

$$\dot{x}_i = \frac{r(h_i)}{K_i + r(h_i)} - \mu_i x_i; \quad h_i = \sum_{j=1}^{n} \theta_{ij} x_j + u_i \tag{7}$$

for $i = 1, 2, \ldots, n$, where θ_{ij} is the ij-th element of the matrix Θ, and gives the regulatory effect of gene j on the expression of gene i (i.e., $\theta_{ij} > 0$, $\theta_{ij} < 0$, and $\theta_{ij} = 0$ represent activation, inhibition, and no interaction, respectively). The expression of each gene can also be activated or inhibited by environmental inputs $\boldsymbol{u} = (u_1, u_2, \ldots, u_n)$. Gene expression follows Michaelis–Menten dynamics with coefficients K_i, and gene product has a degradation rate given by μ_i. In this way, the developmental parameters in this example are θ_{ij}, u_i, K_i, and μ_i for all $i, j = 1, 2, \ldots, n$. For the analyses in this section and the next using the gene-regulatory network, we study the steady state, which we consider maturity of the organism, where gene expression is no longer changing (i.e., $\dot{x}_i = 0$ for all i). We use a bar to denote that a variable corresponds to the steady state (i.e., $\bar{A}$ is the Jacobian at the steady state).

In *Appendix C*, we obtain the Jacobian $\bar{A}$ and the weights $\bar{\boldsymbol{b}}_\lambda$ for each of the developmental parameters, and use them to calculate the sensitivity vector using Eq. **5**. We find that for a given i, the sensitivity vectors $\bar{\boldsymbol{s}}_{\theta_{ij}}$, $\bar{\boldsymbol{s}}_{u_i}$, $\bar{\boldsymbol{s}}_{K_i}$, and $\bar{\boldsymbol{s}}_{\mu_i}$ are totally aligned (i.e., regardless of j) since the weight vectors $\bar{\boldsymbol{b}}$ all have a nonzero value in the i-th position, and zeroes elsewhere. This means that, for example, a perturbation in the environmental input u_i will result in a phenotypic change that is in the same

Fig. 2. Alignment in a reaction–diffusion model. The panel on the *Left* shows in purple the angle between $\boldsymbol{s}_F(t)$ and $\boldsymbol{s}_k(t)$ through development time, and in orange the average angle between $\boldsymbol{s}_k(t)$ and 10 random vectors of the same dimension (1 SD is also plotted but covered by the dots). After a transitory period with oscillations following the introduction of the perturbations, the angle between $\boldsymbol{s}_F$ and $\boldsymbol{s}_k$ is significantly smaller that the angle between random vectors, indicating alignment between the phenotypic effects of perturbing k and F. The three panels to the *Right* show the phenotypes, plotted as the concentration of morphogen 1 with higher concentration in lighter color, for the reference developmental parameters, perturbed k and F, respectively, at developmental time 500. As indicated by the small angle between $\boldsymbol{s}_F$ and $\boldsymbol{s}_k$, the phenotypic effect of the perturbations is similar, resulting in *connected dots* as opposed to the *dotted* pattern in the reference.

direction as a genetic change in any of the elements of the i-th row of Θ. In particular, this phenotypic effect will occur in the direction of vector $col_i(\bar{A}^{-1})$.

We test the analytical predictions by simulating gene networks of five genes and initial concentrations of 0.1 for all genes. We begin by using the sensitivity vectors to predict the phenotypic effects of mutations, which are changes in the elements of the interaction matrix Θ. For this, we generate 100 random gene regulatory networks each with a different reference interaction matrix Θ_k^*. For each network k, we generate 20 mutants by modifying one element of Θ_k^*. We predict the effect of these mutations using Eq. **3** as $\bar{x}^* + \bar{s}_{\theta_{ij}}(\theta_{ij} - \theta_{ij}^*)$, where $\bar{x}^*$ is the steady state of the unperturbed system and $\bar{s}_{\theta_{ij}}$ is as obtained in *Appendix C*. We then compare this prediction with the actual simulated steady state for the mutants.

Fig. 3*A* shows that the formalism based on sensitivity vectors predicts the effect of mutations on the phenotype. As expected, the error in the prediction goes to zero as the perturbations become smaller. Perturbations smaller than 20% in the parameters have median relative error smaller than 3% in the prediction of their phenotypic effect. The predictions for this class of network are robust to larger perturbation, with perturbations in the range of 80 to 100% in the parameters still resulting in predictions with less than 30% median error.

We now turn to the question of alignment between different sources of perturbation. From the results in *Appendix C*, we know that the sensitivity vectors $\bar{s}_{u_i}$ and $\bar{s}_{\theta_{ij}}$ are aligned for any given i, and for all j. This means that perturbing the environmental parameter u_i or perturbing any of the elements in the i-th row of Θ will result in changes in the phenotypes in the same direction. To test this, we generated 100 random reference networks. For each of these reference networks, we introduced genetic and environmental perturbations, in the first row of the reference Θ^* and in u_1^*, respectively. We then simulated the networks until the steady state was reached, and measured the phenotypic effects of the introduced perturbations. Fig. 3*B* shows that the angles between the vectors resulting from these perturbations are significantly smaller than the angles between random vectors. This confirms that the phenotypic effects of these genetic and environmental perturbations are aligned.

From the results in *Appendix C*, we further predict that there should not be alignment between the effects of perturbing environmental parameter u_1 and the elements belonging to the other rows of matrix Θ. *SI Appendix*, Fig. S2 shows that simulated results confirm this prediction from the framework. In this way, the gene regulatory network both shows alignment and unalignment for different pairs of perturbations.

Plasticity and Evolvability. The alignment between the phenotypic effects of genetic and environmental perturbations provides a link between plasticity and evolvability. Indeed, the plastic response of organisms to environmental change can be used to infer what variation can arise through heritable genetic changes, and thus what variation can selection act on.

To study this, we use populations of individuals represented by gene regulatory networks of five genes, where only genes 1 and 2 receive environmental input (i.e., $u_3 = u_4 = u_5 = 0$). We have two sets of 15 populations each that we call *up–down* and *left–right* sets, which differ in how organisms respond plastically to environmental perturbation. As explained in *Materials and Methods*, these populations were obtained by subjecting initially random networks to fluctuating selection tracking an optimum with a correlated environmental input for 500 generations (19).

Fig. 4*A* shows one example population from the *up–down* set in black, and one example population from the *left–right* population in orange. The dots represent the steady states of the phenotypes for the individuals when no environmental input is introduced. The arrows have their origin in these unperturbed reference states, and point in the direction of change when environmental perturbations are introduced. The population plotted in black show large changes in x_4 (i.e., the expression level of gene 4) in response to environmental perturbations, but little change in x_3. The opposite applies to the orange population, which mostly varies in x_3 when environmental perturbations are introduced.

Because we know from the analytical results above that the response to environmental perturbations is aligned with the response to genetic perturbations, we predict that the *left–right* populations should evolve faster, compared to the *up–down* populations, if selected in the direction of increase in x_3 and no change in x_4. We test this by making the populations evolve
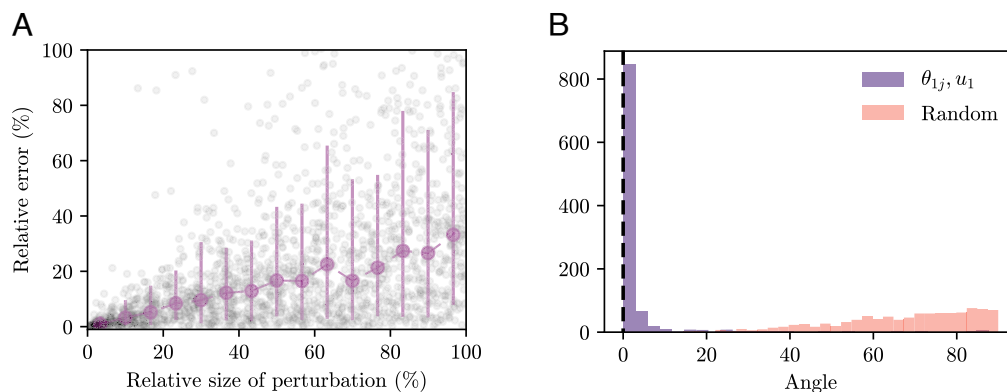
Fig. 3. The general framework predicts the effects of mutations and alignment with environmental perturbations. Panel (*A*) shows the prediction error for the effect of a mutation using the sensitivity vector. The x-axis has the perturbation relative perturbation size $(\theta_{ij} - \theta_{ij}^*)/\theta_{ij}^*$. The relative error was calculated as the difference between predicted change using sensitivity vector and the simulated change, divided by the simulated change. 100 random networks were used as reference and 20 mutants were generated for each reference network. Panel (*B*) shows the alignment between genetic and environmental perturbations in θ_{1j} and u_1 for random j in 1, 2..., 5. The angle between the resulting changes was measured in degrees and plotted as a histogram in purple. As shown in *Appendix C*, the expectation for this angle is zero (i.e., total alignment) as indicated by the dashed line. However, this is only valid for small perturbations, and larger ones may deviate from this expected behavior (see panel *A*) causing some spread in the histogram. Data include 100 reference networks, each with 10 environmental and 10 genetic perturbations introduced. The orange histogram shows the angle between random vectors in five-dimensional morphospace, sampled from a multivariate Gaussian distribution.
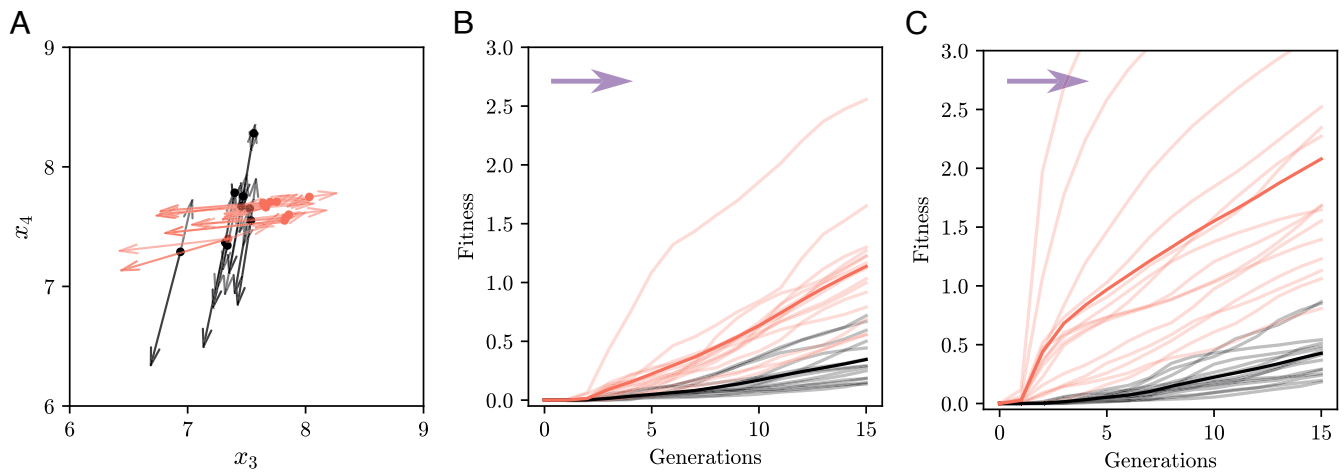
Fig. 4. Plasticity predicts evolvability and this can be used for evolutionary control. Panel (*A*) shows an example population of the *left–right* and *up–down* sets, in orange and black respectively. Dots represent unperturbed individuals (no environmental inputs), and the arrows represent the direction of the change in steady states when an environmental perturbation is introduced in one of the first two states. Panel (*B*) shows evolution for *left–right* and *up–down* populations, toward an optimum located in $(x_3, x_4) = (12.5, 7.5)$ represented with the purple arrow. The *left–right* populations, in orange, outcompete the *up–down*. Transparent lines are the average among the 25 evolutionary lines initiated from a single individual from each of the 15 populations in each set. Panel (*C*) shows that an additional mutational input directly on the first two rows of Θ significantly accelerates evolution toward the optimum for the *left–right* populations.

"to the right," toward an optimum in $(x_3, x_4) = (12.5, 7.5)$. To avoid confounding effects of standing genetic variation, we sampled 25 random individuals from each of the 30 populations (15 *left–right* and 15 *up–down*), and created independent evolutionary lines from 1,000 clones of those randomly sampled individuals (i.e., total of $2 \times 15 \times 25 = 750$ independent evolutionary simulations starting from 1,000 clones each).

Fig. 4*B* confirms that the individuals from the *left–right* populations are consistently faster at evolving "toward the right," to an optimum in $(x_3, x_4) = (12.5, 7.5)$, compared to the individuals from the *up–down* populations. The 15 transparent orange lines correspond to the average of the 25 simulations from each of the 15 *left–right* populations. Similarly, the transparent black lines represent the averages from the 15 *up–down* populations. Total averages are given with fully opaque colors.

For this particular system, we can further use the sensitivity vectors identified in the previous section to accelerate evolution in a desired direction. From the analytical results, and as confirmed with the simulations (Fig. 3*B*), we know that the *i*-th environmental input will be aligned with mutations in the *i*-th row of Θ. Furthermore, we know that the plastic response shown in Fig. 4*A* is generated by perturbation in u_1 and u_2. Therefore, we know that evolution in the desired direction can be accelerated by increasing the mutation rate of the first two rows of Θ.

Fig. 4*C* shows a scenario in which additional mutations are introduced in each generation but only on the first two rows of Θ. For individuals in set *left–right*, many of these mutations will be beneficial since they will be aligned with the plastic response, which itself points toward the optimum at $(x_3, x_4) = (12.5, 7.5)$, as shown in Fig. 4*A*. This results in a marked acceleration of evolution toward the optimum (compare orange lines in panels b and c of Fig. 4). Populations from the set *up–down*, however, cannot benefit from this additional mutational input since we know from Fig. 3*C* that mutations in the first two rows of Θ result in phenotypic changes that do not point toward the optimum for the *up–down* populations. *SI Appendix*, Fig. S3 shows that, analogously, the *up–down* populations outcompete the *left–right* populations if selection is "upward," toward an optimum in

$(x_3, x_4) = (7.5, 12.5)$, and that evolution is accelerated in this direction if we increase the mutational input in the first two rows of Θ for the *up–down*, but not the *left–right* population.

Discussion

In this work, we demonstrate that representing development as a dynamical system provides a theoretical framework to study how generative processes create phenotypic variation, and thus constrain or facilitate adaptive change. The framework is formulated from a bottom–up perspective, utilizing knowledge of developmental dynamics given by function f of Eq. **1** to predict the phenotypic effects of perturbations. This approach contrasts with others that can be described as top–down, such as quantitative genetics, where inferences about underlying mechanisms are made from observational phenotypic data. While these perspectives are not mutually exclusive, they are more suited to different objectives. The bottom–up approach adopted here proves particularly valuable for predicting the relationship between the effects of perturbations of different origins, but cannot be directly used to discern the underlying cause of a given phenotypic change based solely on phenotypic data. It is worth noting that, although beyond the scope of this paper, the framework presented here could be extended to be used in top–down analyses by, for example, inferring sensitivity vectors directly from time series data of developmental perturbations (37).

The general representation of development as a dynamical system captures two general features of generative processes that are lost in static representations that only focus on the outcome of development, but not on how that outcome is constructed (e.g., static maps from genotypes and environments to adult phenotypes). The first property is historicity, which means that the phenotype at any given time is both the effect of earlier, and the cause of later, developmental change. The second property is that all perturbations must affect the developmental process to have an effect on the phenotypes. These two generic features of development are reflected in the elements of the sensitivity vectors, which determine how the phenotype is expected to change as a result of a perturbation during development.

A benefit of this representation of development is that it establishes a formal connection between plasticity and evolvability, understood as the capacity to generate phenotypic variation in response to perturbations of environmental or genetic origin, respectively. The existence of theoretical conditions for when genetic and environmental perturbations result in concordant phenotypic effects indicates that both phenomena ought to be more broadly conceptualized as variational properties that reflect the internal structure of the developmental process (16, 38). This conceptualization has important implications for evolutionary prediction and control, since it suggests that information of plasticity can reveal salient aspects of evolvability, and vice versa. While this link between plasticity and evolvability has been demonstrated before in specific models (17–22), the framework presented here extends this understanding in multiple ways.

First, the general framework based on sensitivity functions allows defining explicit theoretical conditions for when plasticity and evolvability should be aligned. These conditions are general and apply to any system of the general form of Eq. **1**, since they are derived from generic features of development represented as a process. Due to their generality, these conditions open the possibility to scale these results for application in evolutionary prediction and control in diverse systems. Importantly, these conditions apply to any point during development and are not constrained to be applied to the adult. This can be important if, for example, selection occurs during development. A limitation for applying this framework to phenotypic variation in nature is that the developmental function f needs to be known to calculate matrix $A(t)$ and vector $b(t)$. Note however that even if we cannot obtain explicit analytical values for these elements, the general conclusions of the framework still apply.

Second, the framework makes it possible to go beyond the qualitative expectation that genetic and environmental perturbations are to some degree interchangeable in development (e.g., refs. 11 and 39), by making quantitative predictions of the phenotypic effect of perturbation, and of the relationship between different perturbations. As shown in this paper, this information can be exploited to predict responses to selection without an estimate of heritable (co)variance in phenotypes (e.g., as summarized in the G matrix). This is possible because knowledge about plasticity captures properties of developmental systems that carry information about how those systems can accumulate heritable phenotypic variation. While some empirical data (e.g., ref. 13) could be interpreted in this manner, there appears to be no direct test of this prediction. Note, however, that the framework introduced here is only locally valid, meaning that it is predictive of the effects of perturbations of small size. Therefore, predictions of evolvability based on plasticity may only be valid for a limited number of generations after which the sensitivity functions would have to be reidentified since the internal structure of development may have changed.

Finally, the framework reveals how to exploit this alignment for evolutionary control, by accelerating evolution in certain directions through forced mutations predicted to result in adaptive phenotypic changes. More generally, if the sensitivity vectors of multiple perturbations are identified, this means that it is possible to design combinations of perturbations to drive the developmental process in a desired direction. Similar to the other points above, this insight suggests opportunities for empirical investigation of evolvability, which also may have implications in applied fields of biology such as biotechnology.

While so far we have emphasized the alignment between the phenotypic effects of genetic and environmental perturbations, different genetic perturbations can also be aligned with each other (40). In the simulations, this redundancy is evidenced by the fact that mutating any element of the i-th row of Θ in the gene regulatory network or mutating any of the parameters k or F in the reaction–diffusion model, generates concordant phenotypic change. In this way, a population will evolve in the same direction of trait space by accumulating mutations in any of those equivalent elements. This redundancy can explain why genetic changes underlying parallel evolution often fail to be replicated (e.g., ref. 41), since multiple changes at the genetic level can explain the same phenotypic adaptations.

Redundancy ultimately reflects the fact that it is not the identity of any specific gene that matters for the generation of phenotypic variation, but rather the role it plays in the dynamics of the developmental process. This can explain the observation that, despite the multidimensional nature of phenotypic data, it is very often the case that there are only a few effective dimensions of variation (5, 42–44). Indeed, if many perturbations result in concordant phenotypic changes, then phenotypic variation will be restricted to a manifold of lower dimension than the total number of phenotypic variables.

Following this, we should expect that parallel evolution will be explained by a repeatable genetic change only in cases where the effect of perturbing that gene is unaligned with others (i.e., where s_λ points in a direction that is different to the sensitivities of other parameters). This represents a scenario where the perturbed gene plays a distinctive role in developmental dynamics. One possible example of this is the gain and loss of red and yellow carotenoid coloration in diverse vertebrates (e.g., birds, mammals, lizards), which is commonly associated with perturbations in the expression of gene *BCO2* that encodes a carotenoid degradation enzyme (45, 46). This evidence implies that *BCO2* plays a distinctive role in the generation of color, so that perturbations in its functioning have distinctive phenotypic effects. Repeatable genetic changes underlying parallel evolution can thus be used to make inferences about developmental dynamics, guiding future research.

Conclusion

An understanding of evolution is incomplete without a theory of how phenotypic variation is generated in each generation. The representation of development as a process provides the conceptual basis to predict when perturbations of different origins result in similar phenotypic changes. Our results indicate that a promising avenue for future research on the generation of variation will not focus on the specific identity of elements such as genes, but rather focus on how those elements participate in a dynamical process that integrates different sources of information to produce phenotypes.

Materials and Methods

Reaction–Diffusion Simulations. A spatially discretized version of Eq. **6** is implemented (ref. 33). The tissue is composed of a grid of 50 × 50 cells, each having a given amount of the two morphogens, thus resulting in a total of 5,000 states. Diffusion occurs only between neighboring cells and is represented with a discretized version of the Laplacian as commonly done (e.g., ref. 33). Periodic boundary conditions are assumed, so the tissue can be thought of as being mapped to a torus. The first 2,500 states are the concentration of morphogen 1 in the 2,500 cells, while the last 2,500 states correspond to the concentration of morphogen 2. This means that for $i = 1, 2, \ldots, 2,500$, x_i corresponds to concentration of morphogen 1 of the cell located in position $(q + 1, r)$ of the grid

where q and r are the quotient and remainder, respectively, of the division $i \div 50$, where $\div$ represents integer division. Similarly, x_i for $i = 2{,}501, 2{,}502, \ldots,$ 5,000 corresponds to the concentration of morphogen 2 of the cell located in position $(q + 1, r)$ of the grid where q and r are the quotient and remainder, respectively, of the division $(i - 2{,}500) \div 50$. To obtain the sensitivity vectors, we need the Jacobian and the weights. These are obtained by differentiating the discretized equation (33). The Jacobian results in a sparse matrix since only neighboring cells interact (through diffusion). The Jacobian and the weights are given in the accompanying scripts.

Evolutionary Simulations of Gene-Regulatory Networks. Organisms are represented as gene regulatory networks composed of five genes following the developmental function given in Eq. **7** (19, 22). The genotype of each individual is the interaction matrix Θ, where the element θ_{ij} is the regulatory effect of gene j on the expression of gene i, and the phenotype is the gene expression levels at the steady state for the five genes. Organisms reproduce in discrete generations with selection acting on the phenotype. The fitness of each individual is calculated from the Euclidean distance d between the phenotype and the optimum as $exp(-d^2/2)$. Parents are randomly selected in each generation with probability equal to their relative fitness. After the two parents are chosen, the genotype of the offspring is built by recombining the parental genotypes, randomly sampling with equal probability the element θ_{ij} from either parent. Organisms acquire a number of mutations that are Poisson distributed with mean 0.005. Mutations can be of two types: either a change in architecture or a change in the strength of interactions. To implement this, we write the interaction matrix Θ as the element-by-element product of a binary matrix Θ_B, which determines whether gene j regulates gene i or not (with a 1 or 0, respectively), and a matrix Θ_C containing the real-valued strengths of these regulatory influences. With a probability of 0.2, a mutation changes an element of the binary matrix Θ_B, which means adding or removing the regulatory connection between two genes. Alternatively, the mutation changes the weight of a randomly chosen interaction by adding a value from a Gaussian distribution with mean zero and SD of 0.2.

To generate the *up-down* and *left-right* populations (Fig. 4), composed of individuals that have plastic responses in different directions, we evolve populations under fluctuating selection tracking an optimum with a correlated environmental input (see ref. 19). In our simulation, only genes 1 and 2 receive environmental input (i.e., $u_3 = u_4 = u_5 = 0$) and fitness is determined only by genes 3 and 4. We begin by generating 100 random gene networks, such that the steady state for the expression of genes 3 and 4 are in the interval 7.5 ± 2. For each of these random networks, we generate separate populations of clones of 1,000 individuals. These populations of clones are then subject to 500 generations of fluctuating selection, where the values of u_1 and u_2 in each generation determine the position of the optimum in that generation. The environmental inputs u_1 and u_2 are drawn in each generation from a bivariate normal distribution with mean $(0, 0)$ and covariance matrix $[0.2\, 0.18;\, 0.18\, 0.2]$. The first 50 populations of clones were evolved under fluctuating selection where the optimum for x_3 was fixed at 7.5, while the optimum for x_4 was $7.5 + u_1 + u_2$. Analogously, The 50 other populations had fixed selection for $x_4 = 7.5$ and fluctuating in each generation for x_3 following $7.5 + u_1 + u_2$. After the 500 generations of evolution, some of the populations evolved a clear response to environmental inputs that tracked the moving optimum. We refer to as *left-right* populations to the set of 15 populations that evolved to track the optimum that fluctuated for values of x_3 around 7.5, but keeping x_4 fixed at 7.5. Similarly, we call *up-down* populations to the set that evolved tracking an optimum where x_4 fluctuated and x_3 was fixed at 7.5.

Angle between Sensitivity Vectors. The angle $\theta(t)$ between the directions of two sensitivity vectors $s_{\lambda_1}(t)$ and $s_{\lambda_2}(t)$ is defined as the minimum between the angle formed by $s_{\lambda_1}(t)$ and $s_{\lambda_2}(t)$, and the angle formed by $-s_{\lambda_1}(t)$ and $s_{\lambda_2}(t)$. By taking the minimum, we make sure that $\theta(t)$ depends on the direction of the vectors and not the sign. Complete alignment between $s_{\lambda_1}(t)$ and $s_{\lambda_2}(t)$ is then given by $\theta(t) = 0°$, in which case, the sensitivity vectors

have the exact same direction (but possibly different signs). This will be the case if the weights are proportional (i.e., $\tilde{b}_{\lambda_1}(t, \lambda^*) = \alpha \tilde{b}_{\lambda_2}(t, \lambda^*)$ with α constant). More generally, however, we consider that there is evidence for alignment if the angle $\theta(t)$ is significantly smaller, at a given confidence level, than the distribution of angles between independent random vectors in $\mathbb{R}^n$, with n being the number of states. We note that as n becomes larger, the distribution of angles between random vectors in $\mathbb{R}^n$ concentrates around 90°, so random vectors are generally closer to orthogonality in higher dimensional spaces. In this way, $\theta(t) < 90°$ in higher dimensions is a signature of alignment.

Appendixes

Appendix A. Here, we extend the sensitivity analysis to include the possibility that the phenotypes of interest are not directly the states, but rather some function of them. For this, we extend the general equation [**1**] as follows:

$$\dot{x} = f(t, x, \lambda), \quad x(t_0) = x_0, \qquad [\text{A1}]$$

$$y = g(t, x), \qquad [\text{A2}]$$

where $y = (y_1, y_2, \ldots y_m)$ is a vector of m phenotypes of interest, g is a smooth function in x and t, and the rest of the variables are as defined in the main text. We denote by $s_\lambda^y(t)$ the sensitivity vectors that measure the change in the phenotypes y in response to a change in one of the developmental parameters λ. This will be related to the sensitivity of the states $s_\lambda(t)$ defined in Eq. **2** by

$$
\begin{aligned}
s_\lambda^y(t) &= \left.\frac{\partial y(t, x)}{\partial \lambda}\right|_{(t, x^*, \lambda^*)} \\
&= \left.\frac{\partial g(t, x)}{\partial x}\right|_{(t, x^*, \lambda^*)} s_\lambda = C(t, x^*, \lambda^*) s_\lambda, \qquad [\text{A3}]
\end{aligned}
$$

where $C(t, x^*, \lambda^*)$ is a matrix of size $m \times n$ that can be understood as the linear approximation of $g(t, x)$ for small perturbations. The matrix $C(t, x^*, \lambda^*)$ can be calculated in a straightforward manner as the derivative of g with respect to the states, evaluated at time t and at the reference trajectory and parameter value (x^* and λ^*, respectively). The sensitivity vectors defined for the phenotypes y can be used to study alignment between perturbations of different origins in an analogous way to the sensitivities defined for the states. We note that alignment in the states x is sufficient—but not necessary—for alignment in the phenotypes y. In particular, if $C(t, x^*, \lambda^*) = I$ the $n \times n$ identity matrix, then the phenotypes of interest are the states as assumed in the main text. The extension presented here can be used, for example, together with the developmental function f of the gene regulatory network to add an additional functional layer, where the phenotypes are a function of the levels of gene expression.

Appendix B. Here, we obtain an expression for the sensitivity vectors. We begin with the general representation of development as a dynamical system, as given by Eq. **1**. Under the assumption that the developmental function f is smooth, there exists a unique solution $x(t, \lambda)$ for a λ close to the reference value λ^*, which can be obtained as (see ref. 31),

$$x(t, \lambda) = x_0 + \int_{t_0}^{t} f(\tau, x(\tau, \lambda), \lambda) d\tau. \qquad [\text{A4}]$$

We are interested in calculating the sensitivity vector, as defined in Eq. **2**. For this, we take the partial derivative with respect to λ on both sides of Eq. **A4**, which gives

$$s_\lambda(t) = \frac{\partial \boldsymbol{x}(t, \lambda)}{\partial \lambda}$$

$$= \frac{\partial}{\partial \lambda} \left[\boldsymbol{x}_0 + \int_{t_0}^{t} \boldsymbol{f}(\tau, \boldsymbol{x}(\tau, \lambda), \lambda) d\tau \right] \quad [\text{A5}]$$

$$= \int_{t_0}^{t} \left[\frac{\partial \boldsymbol{f}(\tau, \boldsymbol{x}(\tau, \lambda), \lambda)}{\partial \boldsymbol{x}(\tau, \lambda)} s_\lambda(\tau) + \frac{\partial \boldsymbol{f}(\tau, \boldsymbol{x}(\tau, \lambda), \lambda)}{\partial \lambda} \right] d\tau,$$

where we use that the derivative of the initial condition is zero because it does not depend on λ, and the chain rule to obtain the derivative of $\boldsymbol{f}$ with respect to λ.

To obtain an expression for $\dot{\boldsymbol{s}}_\lambda(t)$ of how the sensitivity vector changes in time, we take the partial derivative of Eq. **A5** with respect to time, yielding Eq. **4**.

Appendix C. Here, we derive the equations for the Jacobian, weights, and sensitivity vectors for the developmental parameters of the gene regulatory network. We begin by rewriting Eq. **7** in matrix form. For this, we write $\boldsymbol{h} = \Theta \boldsymbol{x} + \boldsymbol{u}$, and define $\boldsymbol{\kappa} = (K_1, K_2, \ldots, K_n)$ and the $n \times n$ diagonal matrix $M = diag(\mu_1, \mu_2, \ldots, \mu_n)$. This yields

$$\dot{\boldsymbol{x}} = \boldsymbol{f}(t, \boldsymbol{x}, \Theta, \boldsymbol{u}, M, \boldsymbol{\kappa}) = R(\boldsymbol{h}) - M\boldsymbol{x} \quad [\text{A6}]$$

with

$$R(\boldsymbol{h}) = \begin{pmatrix} \frac{r(b_1)}{K_1 + r(b_1)} \\ \vdots \\ \frac{r(b_n)}{K_n + r(b_n)} \end{pmatrix},$$

which follows the form of Eq. **1**, with the developmental parameter vector given by $\lambda = (\Theta, \boldsymbol{u}, M, \boldsymbol{\kappa})$ and reference developmental parameter values given in the vector $\lambda^* = (\Theta^*, \boldsymbol{u}^*, M^*, \boldsymbol{\kappa}^*)$.

The study of alignment in this example is performed at the steady state, with $\dot{x}_i = 0$ for all i. We therefore assume that the reference values for the developmental parameters, given by λ^*, result in a stable system able to reach a steady state $\bar{\boldsymbol{x}}^*$. Further, we assume that $\bar{h}_i > 0$, with the bar indicating the steady state. This allows to replace $r(\bar{h}_i) = \bar{h}_i$. Note that if $\bar{h}_i < 0$, then Eq. **7** reduces to $\dot{x}_i = -\mu_i x_i$ and it can be easily checked that this results in $\bar{\boldsymbol{b}}_{u_i} = \bar{\boldsymbol{b}}_{\theta_{ij}} = \bar{\boldsymbol{b}}_{\mu_i} = \bar{\boldsymbol{b}}_{K_i} = \boldsymbol{0}$. In other words, the steady state is robust to perturbations in the developmental parameters if $\bar{h}_i < 0$.

We obtain the Jacobian,

$$\bar{A} = \frac{\partial \boldsymbol{f}}{\partial \boldsymbol{x}} \bigg|_{\bar{\boldsymbol{x}}^*, \lambda^*} = \frac{\partial \boldsymbol{f}}{\partial \boldsymbol{h}} \frac{\partial \boldsymbol{h}}{\partial \boldsymbol{x}} \bigg|_{\bar{\boldsymbol{x}}^*, \lambda^*} - M^*$$

$$= \begin{pmatrix} \bar{\alpha}_1 & \ldots & 0 \\ \vdots & \ddots & \vdots \\ 0 & \ldots & \bar{\alpha}_n \end{pmatrix} \Theta^* - M^*, \quad [\text{A7}]$$

where $\bar{\alpha}_i = K_i/(K_i + \bar{h}_i)^2$. We now calculate the weights $\bar{\boldsymbol{b}}_\lambda$ as

$$\bar{\boldsymbol{b}}_{u_i} = \frac{\partial \boldsymbol{f}}{\partial u_i} \bigg|_{\bar{\boldsymbol{x}}^*, \lambda^*} = \frac{\partial \boldsymbol{f}}{\partial \boldsymbol{h}} \frac{\partial \boldsymbol{h}}{\partial u_i} \bigg|_{\bar{\boldsymbol{x}}^*, \lambda^*} = [0, \ldots, 0, \bar{\alpha}_i, 0, \ldots, 0]^T,$$

$$\bar{\boldsymbol{b}}_{K_i} = \frac{\partial \boldsymbol{f}}{\partial K_i} \bigg|_{\bar{\boldsymbol{x}}^*, \lambda^*} = [0, \ldots, 0, \bar{\gamma}_i, 0, \ldots, 0]^T,$$

$$\bar{\boldsymbol{b}}_{\mu_i} = \frac{\partial \boldsymbol{f}}{\partial \mu_i} \bigg|_{\bar{\boldsymbol{x}}^*, \lambda^*} = [0, \ldots, 0, \bar{x}_i^*, 0, \ldots, 0]^T,$$

$$\bar{\boldsymbol{b}}_{\theta_{ij}} = \frac{\partial \boldsymbol{f}}{\partial \theta_{ij}} \bigg|_{\bar{\boldsymbol{x}}^*, \lambda^*} = \frac{\partial \boldsymbol{f}}{\partial \boldsymbol{h}} \frac{\partial \boldsymbol{h}}{\partial \theta_{ij}} \bigg|_{\bar{\boldsymbol{x}}^*, \lambda^*} = [0, \ldots, 0, \bar{\alpha}_i \bar{x}_j^*, 0, \ldots, 0]^T,$$

where the nonzero element in each vector is in the i-th position, $\bar{\gamma}_i = -\bar{h}_i/(K_i + \bar{h}_i)^2$ and ^{T} is the transpose. Because the Jacobian is invertible, we can obtain the sensitivity vectors with the simplified expression given in Eq. **5**, as

$$\bar{\boldsymbol{s}}_{u_i} = -\bar{A}^{-1} \bar{\boldsymbol{b}}_{u_i}, \quad \bar{\boldsymbol{s}}_{\theta_{ij}} = -\bar{A}^{-1} \bar{\boldsymbol{b}}_{\theta_{ij}},$$
$$\bar{\boldsymbol{s}}_{\mu_i} = -\bar{A}^{-1} \bar{\boldsymbol{b}}_{\mu_i}, \quad \bar{\boldsymbol{s}}_{K_i} = -\bar{A}^{-1} \bar{\boldsymbol{b}}_{K_i}. \quad [\text{A8}]$$

Thus, the sensitivity functions for u_i, θ_{ij}, μ_i, and K_i are always aligned for a given i and all j. In particular, they point in the direction of the i-th column of $\bar{A}^{-1}$.

1. S. Gilbert, M. Barresi, *Developmental Biology* (Sinauer Associates, Sunderland, MA, ed. 11, 2016).
2. S. H. Rice, A general population genetic theory for the evolution of developmental interactions. *Proc. Natl. Acad. Sci. U.S.A.* **99**, 15518–15523 (2002).
3. M. B. Morrissey, Evolutionary quantitative genetics of nonlinear developmental systems. *Evolution* **69**, 2050–2066 (2015).
4. M. González-Forero, How development affects evolution. *Evolution* **77**, 562–579 (2023).
5. P. Beldade, K. Koops, P. M. Brakefield, Developmental constraints versus flexibility in morphological evolution. *Nature* **416**, 844–847 (2002).
6. P. M. Brakefield, Evo-devo and constraints on selection. *Trends Ecol. Evol.* **21**, 362–368 (2006).
7. F. Galis, J. W. Arntzen, R. Lande, Dollo's law and the irreversibility of digit loss in Bachia. *Evolution* **64**, 2466–2476 (2010).
8. R. Lande, Quantitative genetic analysis of multivariate evolution, applied to brain: Body size allometry. *Evolution* **33**, 402–416 (1979).
9. A. G. Jones, S. J. Arnold, R. Bürger, Stability of the g-matrix in a population experiencing pleiotropic mutation, stabilizing selection, and genetic drift. *Evolution* **57**, 1747–1760 (2003).
10. J. M. Cheverud, A comparison of genetic and phenotypic correlations. *Evolution* **42**, 958–968 (1988).
11. M. J. West-Eberhard, *Developmental Plasticity and Evolution* (Oxford University Press, 2003).
12. H. F. Nijhout, Colour pattern modification by coldshock in Lepidoptera. *Development* **81**, 287–305 (1984).
13. D. W. Noble, R. Radersma, T. Uller, Plastic responses to novel environments are biased towards phenotype dimensions with high additive genetic variation. *Proc. Natl. Acad. Sci. U.S.A.* **116**, 13452–13461 (2019).
14. M. Kirschner, J. Gerhart, Evolvability. *Proc. Natl. Acad. Sci. U.S.A.* **95**, 8420–8427 (1998).
15. L. M. Chevin, C. Leung, A. Le Rouzic, T. Uller, Using phenotypic plasticity to understand the structure and evolution of the genotype–phenotype map. *Genetica* **150**, 209–221 (2022).
16. G. P. Wagner, L. Altenberg, Perspective: Complex adaptations and the evolution of evolvability. *Evolution* **50**, 967–976 (1996).
17. L. W. Ancel, W. Fontana, Plasticity, evolvability, and modularity in RNA. *J. Exp. Zool.* **288**, 242–283 (2000).
18. C. Espinosa-Soto, O. C. Martin, A. Wagner, Phenotypic plasticity can facilitate adaptive evolution in gene regulatory circuits. *BMC Evol. Biol.* **11**, 1–14 (2011).
19. J. A. Draghi, M. C. Whitlock, Phenotypic plasticity facilitates mutational variance, genetic variance, and evolvability along the major axis of environmental variation. *Evolution* **66**, 2891–2902 (2012).
20. C. Furusawa, K. Kaneko, Global relationships in fluctuation and response in adaptive evolution. *J. R. Soc. Interface* **12**, 20150482 (2015).
21. J. van Gestel, F. J. Weissing, Regulatory mechanisms link phenotypic plasticity to evolvability. *Sci. Rep.* **6**, 24524 (2016).
22. M. Brun-Usan, A. Rago, C. Thies, T. Uller, R. A. Watson, Development and selective grain make plasticity 'take the lead' in adaptive evolution. *BMC Ecol. Evol.* **21**, 1–17 (2021).
23. S. Kondo, T. Miura, Reaction–diffusion model as a framework for understanding biological pattern formation. *Science* **329**, 1616–1620 (2010).
24. A. Wagner, Evolution of gene networks by gene duplications: A mathematical model and its implications on genome organization. *Proc. Natl. Acad. Sci. U.S.A.* **91**, 4387–4391 (1994).
25. I. Salazar-Ciudad, J. Jernvall, A computational model of teeth and the developmental origins of morphological variation. *Nature* **464**, 583–586 (2010).

26. R. C. Lewontin, The organism as the subject and object of evolution. *Scientia* **77**, 65 (1983).

27. P. Alberch, From genes to phenotype: Dynamical systems and evolvability. *Genetica* **84**, 5–11 (1991).

28. G. S. Stent, Thinking in one dimension: The impact of molecular biology on development. *Cell* **40**, 1–2 (1985).

29. E. A. Bassett, V. A. Wallace, Cell fate determination in the vertebrate retina. *Trends Neurosci.* **35**, 565–573 (2012).

30. W. W. Burggren, C. A. Mueller, Developmental critical windows and sensitive periods as three-dimensional constructs in time and space. *Physiol. Biochem. Zool.* **88**, 91–102 (2015).

31. H. Khalil, *Nonlinear Systems* (Pearson Education, ed. 3, 2002).

32. A. M. Turing, The chemical basis of morphogenesis. *Bull. Math. Biol.* **52**, 153–197 (1990).

33. S. Sick, S. Reinker, J. Timmer, T. Schlake, WNT and DKK determine hair follicle spacing through a reaction–diffusion mechanism. *Science* **314**, 1447–1450 (2006).

34. J. B. Green, J. Sharpe, Positional information and reaction–diffusion: Two big ideas in developmental biology combine. *Development* **142**, 1203–1211 (2015).

35. P. Gray, S. K. Scott, Archetypal response patterns for open chemical systems with two components. *Philos. Trans. R. Soc. Lond. Ser. A: Phys. Eng. Sci.* **332**, 69–87 (1990).

36. J. Raspopovic, L. Marcon, L. Russo, J. Sharpe, Digit patterning is controlled by a Bmp-Sox9-Wnt Turing network modulated by morphogen gradients. *Science* **345**, 566–570 (2014).

37. L. Milocco, T. Uller, A data-driven framework to model the organism–environment system. *Evol. Dev* **25**, 439–450 (2023).

38. I. Salazar-Ciudad, Developmental constraints vs. variational properties: How pattern formation can help to understand evolution and development. *J. Exp. Zool. Part B: Mol. Dev. Evol.* **306**, 107–125 (2006).

39. J. M. Cheverud, Phenotypic, genetic, and environmental morphological integration in the cranium. *Evolution* **36**, 499–516 (1982).

40. W. Pitchers *et al.*, A multivariate genome-wide association study of wing shape in *Drosophila melanogaster*. *Genetics* **211**, 1429–1447 (2019).

41. K. Pelletier *et al.*, Complexities of recapitulating polygenic effects in natural populations: Replication of genetic effects on wing shape in artificially selected and wild-caught populations of *Drosophila melanogaster*. *Genetics* **224**, iyad050 (2023).

42. D. Houle, G. H. Bolstad, K. van der Linde, T. F. Hansen, Mutation predicts 40 million years of fly wing evolution. *Nature* **548**, 447–450 (2017).

43. V. Alba, J. E. Carthew, R. W. Carthew, M. Mani, Global constraints within the developmental program of the Drosophila wing. *eLife* **10**, e66750 (2021).

44. P. T. Rohner, D. Berger, Developmental bias predicts 60 million years of wing shape evolution. *Proc. Natl. Acad. Sci. U.S.A.* **120**, e2211210120 (2023).

45. D. I. Våge, I. A. Boman, A nonsense mutation in the beta-carotene oxygenase 2 (BCO2) gene is tightly associated with accumulation of carotenoids in adipose tissue in sheep (*Ovis aries*). *BMC Genet.* **11**, 1–6 (2010).

46. P. Andrade *et al.*, Regulatory changes in pterin and carotenoid genes underlie balanced color polymorphisms in the wall lizard. *Proc. Natl. Acad. Sci. U.S.A.* **116**, 5633–5642 (2019).

47. L. Milocco, lisandromilocco/DevDyn. GitHub. https://github.com/lisandromilocco/DevDyn. Deposited 12 March 2024.